

ter chromatids still connected. These cells nevertheless re-replicate their DNA, resulting in the formation of diplochromosomes in the subsequent mitosis (Fig. 4C). Repeated cycles of abortive mitosis and DNA re-replication may cause formation of the polyploid or multinucleate cells observed by FACS and microscopy (Fig. 3). Paradoxically, spread diplochromosomes typically appeared as pairs of chromosomes whose centromeric regions were not connected (Fig. 4C). Their nonrandom parallel orientation on the coverslips can only be explained, however, by assuming that all four chromatids had been connected by cohesion prior to the hypotonic spreading procedure.

Our results suggest that cohesin cleavage is essential for sister chromatid separation and cytokinesis, even though only a minor amount of SCC1 is cleaved in mitosis (9). It is therefore likely that the anaphase defects of cells in which separase activity is compromised by securin overexpression or deletion are similarly caused by defects in SCC1 cleavage (22, 23). Because SCC1 cleavage coincides with the disappearance of cohesin from centromeres (9), SCC1 cleavage may preferentially dissolve cohesion at centromeres. It is possible that the cytokinesis defects induced by noncleavable cohesin are caused by a mechanical inability of the cleavage furrow to cut through chromosomes remaining in the furrow plane. Alternatively, it is conceivable that a surveillance mechanism prevents cytokinesis in the presence of unseparated sister chromatids.

Our observations also support the notion that sister separation is essential neither for cyclin B destruction and exit from mitosis nor for DNA re-replication in the next cell cycle (2, 4–8, 21) — and is also not necessary for relocalization of Aurora-B from centromeres to the spindle midzone. Naturally occurring defects in separase activation and SCC1 cleavage would therefore not simply block cell cycle progression, but could instead cause chromosome non-disjunction events that could subsequently cause continued chromosomal instability by initiating chromosome breakage-fusion-bridge cycles (24). It will therefore be of interest to determine if defects in separase regulation contribute to the genomic instability observed in human tumors.

References and Notes

1. K. Nasmyth, J. M. Peters, F. Uhlmann, *Science* **288**, 1379 (2000).
2. F. Uhlmann, F. Lottspeich, K. Nasmyth, *Nature* **400**, 37 (1999).
3. F. Uhlmann, D. Wernic, M. A. Poupart, E. V. Koonin, K. Nasmyth, *Cell* **103**, 375 (2000).
4. O. Cohen-Fix, J. M. Peters, M. W. Kirschner, D. Koshland, *Genes Dev.* **10**, 3081 (1996).
5. H. Funabiki *et al.*, *Nature* **381**, 438 (1996).
6. R. Ciosk *et al.*, *Cell* **93**, 1067 (1998).
7. H. Zou, T. J. McGarry, T. Bernal, M. W. Kirschner, *Science* **285**, 418 (1999).
8. O. Leisemann, A. Herzig, S. Heidmann, C. F. Lehner, *Genes Dev.* **14**, 2192 (2000).
9. I. C. Waizenegger, S. Hauf, A. Meinke, J. M. Peters, *Cell* **103**, 399 (2000).

10. A. Losada, M. Hirano, T. Hirano, *Genes Dev.* **12**, 1986 (1998).
11. I. Sumara, E. Vorlaufer, C. Gieffers, B. H. Peters, J. M. Peters, *J. Cell Biol.* **151**, 749 (2000).
12. S. B. Buonomo *et al.*, *Cell* **103**, 387 (2000).
13. T. Tomonaga *et al.*, *Genes Dev.* **14**, 2757 (2000).
14. S. Hauf, I. C. Waizenegger, J.-M. Peters, data not shown.
15. G. Alexandru, F. Uhlmann, K. Mechtler, M. Poupart, K. Nasmyth, *Cell* **105**, 459 (2001).
16. Supplementary material is available at Science Online at www.sciencemag.org/cgi/content/full/293/5533/1320/DC1.
17. E. Vorlaufer, J. M. Peters, *Mol. Biol. Cell* **9**, 1817 (1998).
18. M. Yanagida, *Trends Cell Biol.* **8**, 144 (1998).
19. E. A. Nigg, *Nature Rev. Mol. Cell Biol.* **2**, 21 (2001).
20. T. Kanda, K. F. Sullivan, G. M. Wahl, *Curr. Biol.* **8**, 377 (1998).
21. R. Stratmann, C. F. Lehner, *Cell* **84**, 25 (1996).
22. A. Zur, M. Brandeis, *EMBO J.* **20**, 792 (2001).
23. P. V. Jallepalli *et al.*, *Cell* **105**, 445 (2001).
24. B. McClintock, *Cold Spring Harbor Symp. Quant. Biol.* **9**, 72 (1941).
25. Single-letter abbreviations for the amino acid residues are as follows: A, Ala; C, Cys; D, Asp; E, Glu; F, Phe; G, Gly; H, His; I, Ile; K, Lys; L, Leu; M, Met; N, Asn; P, Pro; Q, Gln; R, Arg; S, Ser; T, Thr; V, Val; W, Trp; and Y, Tyr. X indicates any residue.
26. We thank K. Paiha and P. Steinlein for help with microscopy and FACS, A. H. F. M. Peters for advice on chromosome spreading, A. Kromminga for CREST serum, N. Redemann for Polo-like kinase, and T. Kanda and G. Wahl for the H2B-GFP construct. We are grateful to K. Nasmyth and members of the Peters lab for critically reading the manuscript. Supported by Boehringer Ingelheim and by a grant from the Austrian Science Fund (FWF P13865-BIO). S.H. was supported by a post-doctoral fellowship from the Deutscher Akademischer Auslandsdienst (DAAD).

5 April 2001; accepted 26 June 2001

Vascular Abnormalities and Deregulation of VEGF in *Lkb1*-Deficient Mice

Antti Ylikorkala,^{1*} Derrick J. Rossi,^{1*} Nina Korsisaari,¹ Keijo Luukko,² Kari Alitalo,^{1,3} Mark Henkemeyer,⁴ Tomi P. Mäkelä^{1,3,†}

The *LKB1* tumor suppressor gene, mutated in Peutz-Jeghers syndrome, encodes a serine/threonine kinase of unknown function. Here we show that mice with a targeted disruption of *Lkb1* die at midgestation, with the embryos showing neural tube defects, mesenchymal cell death, and vascular abnormalities. Extraembryonic development was also severely affected; the mutant placentas exhibited defective labyrinth layer development and the fetal vessels failed to invade the placenta. These phenotypes were associated with tissue-specific deregulation of vascular endothelial growth factor (VEGF) expression, including a marked increase in the amount of VEGF messenger RNA. Moreover, VEGF production in cultured *Lkb1*^{-/-} fibroblasts was elevated in both normoxic and hypoxic conditions. These findings place *Lkb1* in the VEGF signaling pathway and suggest that the vascular defects accompanying *Lkb1* loss are mediated at least in part by VEGF.

Germ line mutations of the *LKB1* gene cause Peutz-Jeghers syndrome, which is characterized by gastrointestinal polyposis, abnormal melanin pigmentation, and increased risk of cancer (1). The *Lkb1* gene encodes a serine/threonine kinase of unknown function with no identified in vivo substrates and a ubiquitous expression pattern during mouse development (2). To study the function of *Lkb1*,

we generated *Lkb1*-deficient mice.

Two independent gene-targeting strategies were used to functionally disrupt *Lkb1* in the murine germ line (3, 4). In *Lkb1* heterozygous (*Lkb1*^{+/-}) intercrosses, both *Lkb1*^{+/+} (n = 87) and *Lkb1*^{+/-} (n = 177) animals were observed at expected frequencies, whereas no *Lkb1*^{-/-} animals were obtained. Analysis of *Lkb1*^{-/-} embryos throughout embryonic development revealed no abnormalities before embryonic day 7.5 (E7.5), and most embryos appeared to develop normally up to E8.0. Macroscopic analysis of *Lkb1*^{-/-} embryos beyond E8.25 revealed multiple abnormalities, including a failure of the embryo to turn, a defect in neural tube closure, and a hypoplastic or absent first branchial arch (Fig. 1A). No viable embryos were recovered after E11.0, indicating that *Lkb1* is essential for embryonic development.

Whole-mount in situ hybridization was used to study the integrity of various developmental

¹Molecular and Cancer Biology Program, Haartman Institute and Biomedicum Helsinki, Post Office Box 63, University of Helsinki, Helsinki 00014, Finland. ²Department of Anatomy and Cell Biology, University of Bergen N-5009 Bergen, Norway. ³Helsinki University Central Hospital Laboratory Diagnostics, Post Office Box 401, Helsinki 00029 HYKS, Finland. ⁴Center for Developmental Biology, University of Texas Southwestern Medical Center, Dallas, TX 75235–9133, USA.

*These authors contributed equally to this work.

†To whom correspondence should be addressed. E-mail: tomi.makela@helsinki.fi

REPORTS

lineages in the *Lkb1*^{-/-} embryos at E8.5 and E9.5 (5). The expression of the mesodermal marker brachyury (6) (*T*; Fig. 1B) showed that although the notochord developed along the full length of the anterior/posterior axis in the mutant embryos, it was misaligned and contorted. This was accompanied by defective somitogenesis, which resulted in dysmorphic protrusive somites (arrowhead in Fig. 1A), which failed to

express engrailed 1 (7) at E9.5 (*En1*; Fig. 1C). No pronounced changes in the expression of *Wnt3A* (E8.5), *Fgf8* (E9.0), or *Krox-20* (E9.0) were noted (8), suggesting that there was normal development of the mesoderm of the tail bud, forebrain, and primitive streak, and normal segmentation of the hindbrain.

Mutant embryos at E9.25 had a translucent appearance, suggesting the possibility of vascu-

lar defects (Fig. 1A). To visualize endothelial cells, we subjected E8.5 and E9.5 embryos to whole-mount immunostaining for the platelet endothelial cell adhesion molecule-1 (PECAM-1) (9). Both mutant and wild-type embryos developed a paired dorsal aorta, but by E8.5, the mutant aorta was thin and discontinuous, particularly in the anterior part of the vessel (arrowhead in Fig. 2A). At E9.5, the lumen of the mutant aorta remained thin (arrows in Fig. 2B), with intersomitic branches terminating prematurely in the mesenchyme.

Histological sections of E9.5 *Lkb1*^{-/-} neural folds often revealed large cystic degenerations near the dorsal aorta that occasionally contained embryonic blood cells (asterisks in Fig. 2C). Additionally, the surrounding cephalic mesenchyme had a lower cell density and fewer developing capillaries than controls (Fig. 2C). The decreased cell density was due to increased cell death in the mesenchyme as determined by terminal deoxynucleotidyl transferase-mediated dUTP nick end-labeling (TUNEL) (Fig. 2D) (10). This phenotype was limited to the E9.5 embryos; the E8.5 embryos showed similar numbers of TUNEL-positive nuclei regardless of genotype (8).

In addition to the endothelial and mesenchymal defects, abnormalities were also observed in vascular smooth muscle cells (VSMCs) in E9.5 embryos as revealed by

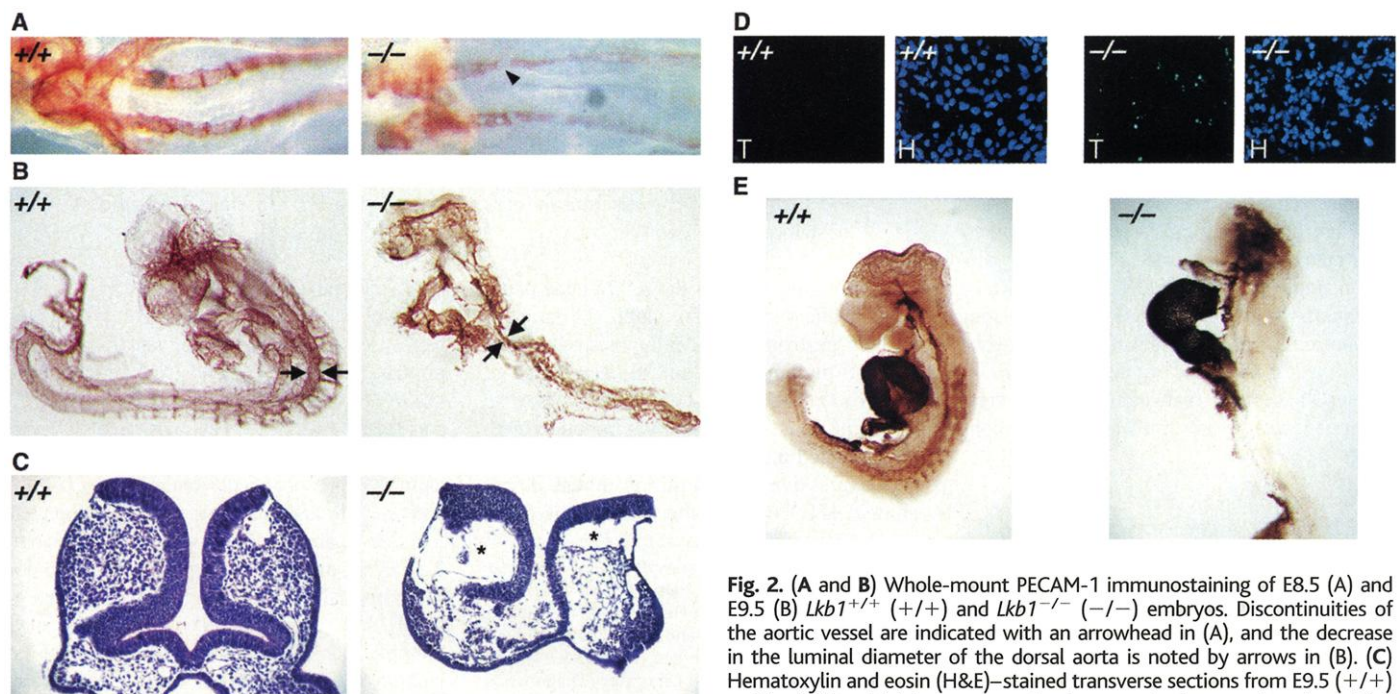
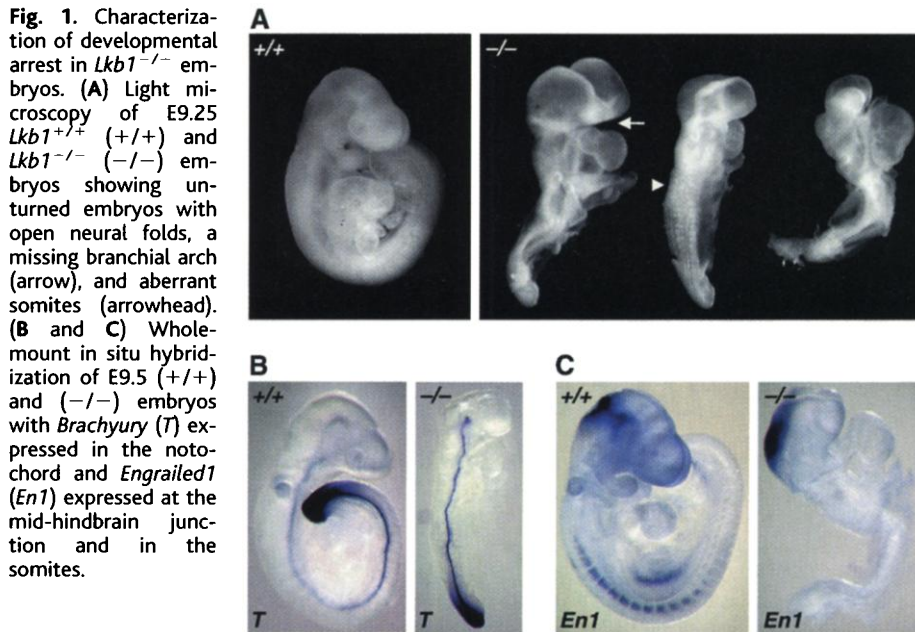


Fig. 2. (A and B) Whole-mount PECAM-1 immunostaining of E8.5 (A) and E9.5 (B) *Lkb1*^{+/+} (+/+) and *Lkb1*^{-/-} (-/-) embryos. Discontinuities of the aortic vessel are indicated with an arrowhead in (A), and the decrease in the luminal diameter of the dorsal aorta is noted by arrows in (B). (C) Hematoxylin and eosin (H&E)-stained transverse sections from E9.5 (+/+) and (-/-) head folds demonstrating large cystic degenerations (asterisks) and aberrant mesenchyme in the mutant. (D) Cell death in E9.5 (+/+) and (-/-) cephalic mesenchyme as assessed by TUNEL labeling (T). Sections were counterstained with Hoechst (H). (E) Whole-mount smooth-muscle actin immunostaining of E9.5 (+/+) and (-/-) embryos. The absence of signal surrounding the mutant dorsal aorta and the ectopic VSMC signal in the head folds of the mutant embryo is apparent.

REPORTS

staining with antibodies to smooth-muscle actin (Sm-A) (9). Although Sm-A expression in the developing heart was comparable in mutant and control embryos (Fig. 2E), *Lkb1*^{-/-} embryos showed a complete absence of VSMC staining in the dorsal aorta and somites. In addition, an unusual, strong ectopic Sm-A signal was detected in head folds of mutant embryos (Fig. 2E). This ectopic VSMC staining was evenly distributed within the cephalic mesenchyme and did not appear to contribute to the supportive vascular structures (8). These observations suggest that abnormal VSMC development may be one of the factors contributing to the vascular and mesenchymal defects.

Analysis of extraembryonic tissues at E9.5 revealed that the mutant yolk sacs failed to develop large vitelline vessels and an extensive capillary network (Fig. 3A), and they contained large cavities that sequestered vast pools of embryonic blood (arrow in Fig. 3A). There were rudimentary vessels between parietal and visceral leaves of the yolk sac, which were congested by nucleated embryonic blood cells (Fig. 3B). The vitelline artery was completely atretic in *Lkb1*^{-/-} yolk sacs, effectively disconnecting the embryo from the yolk sac (vitelline) circulation.

High expression of *Lkb1* mRNA in the placenta (4) suggested that placental development might also be compromised in the *Lkb1*

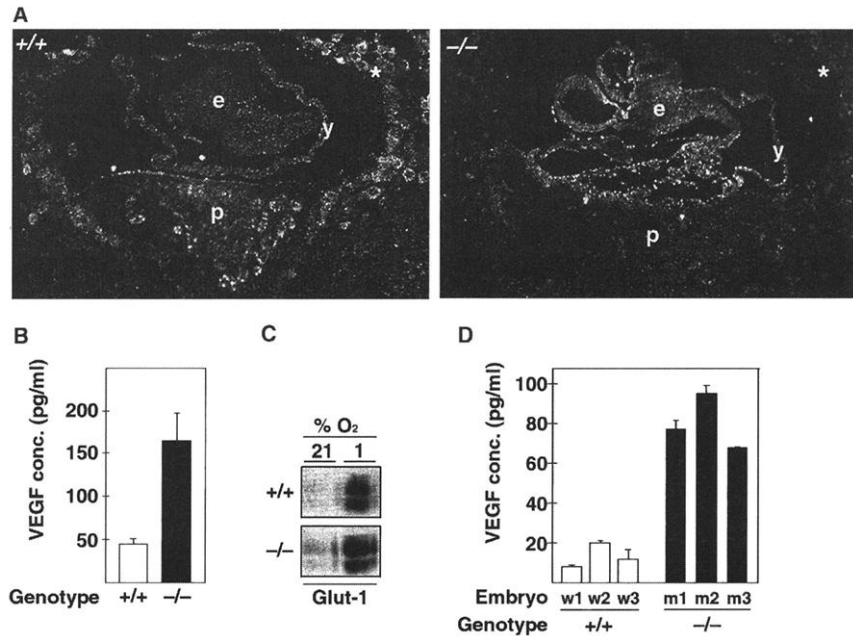


Fig. 4. Deregulation of *VEGF* expression after loss of *Lkb1* in embryos (A) and in cell culture (B and D). (A) *VEGF* in situ hybridization analysis of cross sections of E9.5 (+/+) and (-/-) conceptuses with embryo (e), yolk sac (y), placenta (p), and trophoblast giant cells (asterisks) indicated in the dark-field images ($\times 20$). (B) *VEGF* levels in supernatants of (+/+) and (-/-) MEF cultures subjected to 1% O₂ for 24 hours. Error bars indicate the standard deviation in independent *VEGF* ELISA measurements. (C) Western blot analysis of glucose transporter 1 (*Glut-1*) in normoxia (21% O₂) and hypoxia (1% O₂) in lysates from (+/+) and (-/-) MEFs, showing comparable induction of *Glut-1* in both. (D) *VEGF* levels in supernatants of wild-type (w1, w2, w3) and mutant (m1, m2, m3) cultures, each generated from independent littermate embryos. Error bars as in (B).

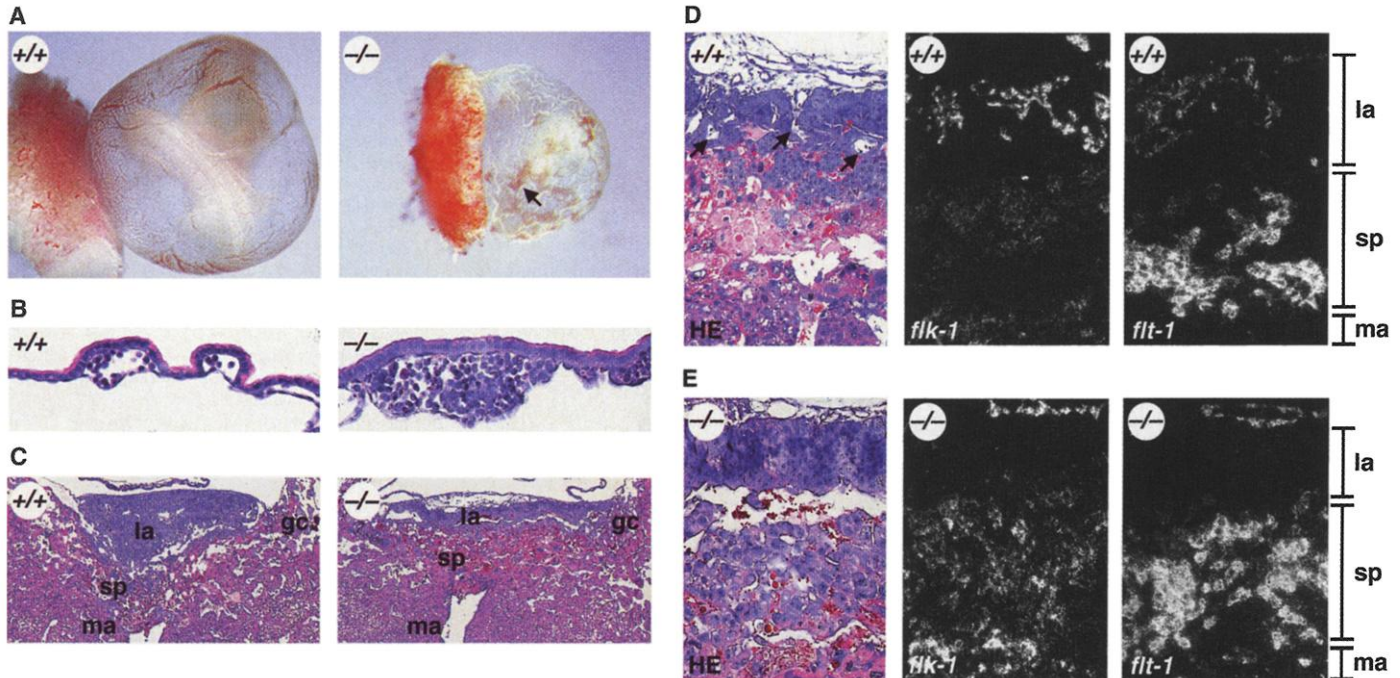


Fig. 3. Characterization of E9.5 *Lkb1*^{-/-} and *Lkb1*^{+/+} yolk sacs (A and B) and placentas (A, C to E). (A) Yolk sac vasculature of E9.5 (+/+) and (-/-) conceptuses. The rudimentary vasculature, lack of vitelline vessels, and pools of embryonic blood (arrow) are apparent in the mutant. (B) Cross section of H&E-stained wild-type yolk sac, demonstrating congestion of mutant blood islands with nucleated embryonic blood cells (-/-). Magnification, $\times 400$. (C) Low-power ($\times 40$) cross section of (+/+) and (-/-) placentas with labyrinthine (la), giant cell (gc), spongio

(sp), and maternal (ma) layers, demonstrating shallow invasion of decidua and rudimentary labyrinth layer in the mutant. (D and E) High magnification ($\times 100$) of fetal vessels invading the labyrinth layer in (+/+) [arrows in (D), HE], but not in (-/-) placentas. In situ hybridization of adjacent sections with *flk-1* and *flt-1*, showing the absence of *flk-1* in the mutant labyrinth layer (E) [*flk-1*, la] and comparable expression of *flt-1* in wild-type and mutant spongiotrophoblast layers [*flt-1* in (D) and (E)].

conceptuses. Mutant placentas at E9.5 were oedematous, hemorrhagic, and small in diameter (Fig. 3A). The connection between placenta and the embryo (chorio-allantoic fusion) in *Lkb1*^{-/-} conceptuses was delayed compared with controls, but had occurred by E9.5. However, invasion of embryonic blood vessels (arrows in Fig. 3D) into the placenta did not occur in the mutant (Fig. 3E), and embryo-derived (nucleated) erythrocytes were not detected in mutant placentas. The lacunae in *Lkb1*^{-/-} placentas were abnormally congested with maternal erythrocytes and by E10.5 the blood lacunae had ruptured, leading to massive hemorrhaging. In situ hybridization (10) with a probe for VEGF receptor *flt-1*, which detects migrating allantoic vessels in the placenta (11), confirmed the lack of fetal blood vessels in the rudimentary labyrinth layer (la in Fig. 3E). The spongioroblast layer (sp in Fig. 3, D and E) was less organized in the mutant and contained more VEGF receptor *flt-1* (12) negative giant cells than did the controls. As expected, *flt-1* was expressed in the maturing fetal vessels in the labyrinth layer of the wild-type (la in Fig. 3D) but not in the mutant placentas (Fig. 3E). The spongioroblast marker *snai* and the vascular development marker *Tgf-β₁* were expressed normally in the mutant placentas (8).

In the embryo *flk-1*, *flt-1*, *snai*, and *Tgf-β₁* were expressed at comparable levels (8). However, expression of another key regulator of embryonic vascular development, *VEGF* (13, 14), was found to be deregulated in both the embryonic and extraembryonic compartments at E8.5 (8) and E9.5 (Fig. 4A). The *Lkb1*^{-/-} placentas exhibited markedly diminished *VEGF* mRNA expression (p in Fig. 4A) particularly in the trophoblast giant cells (asterisk in Fig. 4A), whereas the *Lkb1*^{-/-} embryos expressed abnormally elevated levels of *VEGF* in several tissues including the mesenchyme, heart, and yolk sac (y and e in Fig. 4A).

To investigate whether *Lkb1* directly regulates VEGF expression, we isolated primary mouse embryonic fibroblasts (MEFs) from E8.5 wild-type and mutant embryos, expanded them in culture for 2 weeks (15), and then subjected the cells to hypoxic conditions (1% O₂) for 24 hours to induce VEGF expression (16). Analysis of VEGF levels in culture supernatants (Fig. 4B) revealed that the mutant MEFs produced significantly higher levels of VEGF than controls (165.0 ± 31.9 versus 44.5 ± 6.2 pg/ml, respectively) in hypoxic conditions.

The elevated VEGF levels in the mutant MEF could have resulted from an increased HIF-1-mediated hypoxia response or from a deregulation of basal VEGF expression. Because the HIF-1 levels remained undetectable in MEFs, we assayed the expression of *Glut1* (17), a HIF-1-responsive marker of hypoxia, before and after exposure of the cells to hypoxia (Fig. 4C). There was a comparable induction of *Glut1* in wild-type and mutant MEFs, suggesting that

loss of *Lkb1* had not changed the HIF-1 response to hypoxia. In addition, VEGF secretion in normoxic conditions was significantly higher in the mutant than in wild-type MEFs (80.3 ± 13.9 versus 12.3 ± 5.4 pg/ml) (Fig. 4D). These results indicate that loss of *Lkb1* leads to increased basal and induced expression of VEGF in fibroblasts.

In summary, we have demonstrated that disruption of *Lkb1* results in multiple developmental defects resulting in embryonic lethality and establishes *Lkb1* as a critical regulator of mammalian vascular development. This phenotype was associated with tissue-specific deregulation of *VEGF* expression. Whereas *VEGF* was significantly down-regulated in extraembryonic tissues, embryonic *VEGF* was markedly up-regulated. Disruption of the murine *VHL* tumor suppressor gene exhibits a similar extraembryonic down-regulation of *VEGF* (18), and while the expression of *VEGF* in *VHL*^{-/-} embryos has not been reported, *VHL* loss in other systems has been found to lead to up-regulation of *VEGF* (19, 20). Exploring well-characterized pathways regulating *VEGF* expression, we found unexpectedly that HIF-1 does not appear to play a role in *Lkb1*-mediated *VEGF* expression based on unaltered *Glut-1* levels (Fig. 4C) and undetectable HIF-1α in *Lkb1*^{-/-} MEF cultures (8). Similarly, neither the p42/44^{MAPK} nor the p38 kinase pathways appear to be deregulated based on unaltered levels of activated p42/44^{MAPK} or p38 kinases in *Lkb1*^{-/-} MEF cultures (8).

Our findings have established a genetic link between *Lkb1* and *VEGF* regulation, thereby placing *Lkb1* in the VEGF signaling pathway. This suggests that the vascular defects accompanying *Lkb1* loss that we describe are mediated at least in part by VEGF, thereby providing a basis for the vascular phenotype. Most important, our results also provide a rationale for the increased risk of cancer incidence in Peutz-Jeghers patients (21) by demonstrating that loss of *Lkb1* confers an increased angiogenic potential in certain cell types by up-regulation of VEGF.

References and Notes

1. A. Hemminki et al., *Nature* **391**, 184 (1998).
2. K. Luukko, A. Ylikorkala, M. Tiainen, T. P. Makela, *Mech. Dev.* **83**, 187 (1999).
3. Two independent targeting strategies were used. The first resulted in a deletion of genomic sequences encompassing exons 2 to 7 (out of a total of 10); the second, based on Cre/LoxP methodology, resulted in the inversion of these sequences. In both cases, we used a 6.3-kb Nsi I-Hind III (5') fragment and 2.0-kb Bam HI-Bam HI (3') fragment of genomic sequence. Positive (PGK-Neomycin) and negative (PGK-HSV-tk) selection markers were used in both strategies. The target vectors were electroporated into embryonic stem (ES) cells and correctly targeted clones were identified by Southern blotting with 5' and 3' external probes. ES cell clones were injected into C57BL/6 blastocysts. Several chimeric offspring were found to transmit targeted alleles in the germ line. Germ line inactivation of *Lkb1* with LoxP/Cre was achieved by crossing targeted animals to PGK-Cre mice (22). Stable inversion of the targeted sequences was then achieved by breeding the PGK-Cre transgene out of subsequent generations. *Lkb1*^{-/-} animals ob-

tained with both strategies were found to have identical phenotypes, and both were used in this study.

4. Supplementary Web material is available on Science Online at www.sciencemag.org/cgi/content/full/293/5533/1323/DC1.
5. For whole-mount in situ hybridization, embryos were fixed overnight in 4% paraformaldehyde, bleached for 5 hours in 7% H₂O₂-93% methanol, treated with 5 μg/ml proteinase K, and postfixed in 4% paraformaldehyde-0.2% glutaraldehyde. Overnight hybridization at 63°C with digoxigenin-uridine triphosphate-labeled antisense probe in 50% formamide, 0.75% NaCl, 10 mM Pipes (pH 6.8), 1 mM EDTA, 100 μg/ml tRNA, 0.05% heparin, 0.1% bovine serum albumin, 1% SDS was followed by ribonuclease A-ribonuclease T1 treatment, extensive washes, and blocking in 10% goat serum. Embryos were incubated overnight (4°C) with alkaline phosphatase (AP)-conjugated anti-digoxigenin (Roche Molecular Biochemicals), and AP activity was then detected with BM purple.
6. D. G. Wilkinson, S. Bhatt, B. G. Herrmann, *Nature* **343**, 657 (1990).
7. A. L. Joyner, G. R. Martin, *Genes Dev.* **1**, 29 (1987).
8. A. Ylikorkala et al., data not shown.
9. For whole-mount immunostainings, E8.5 or E9.5 embryos were fixed in 4% paraformaldehyde, bleached for 5 hours in 5% H₂O₂-95% methanol, and blocked overnight (4°C) in phosphate-buffered saline containing 3% milk and 0.1% Triton X-100. After an overnight (4°C) incubation with primary antibodies (PECAM-1, Pharming; smooth-muscle actin, Sigma), the embryos were treated with peroxidase-conjugated secondary antibodies and developed in 3,3'-diaminobenzidine tetrahydrochloride (Sigma).
10. TUNEL labeling and in situ hybridization were performed on paraffin-embedded and paraformaldehyde-fixed 7-μm tissue sections. TUNEL analysis was performed as instructed by the manufacturer (In Situ Cell Death Detection Kit, Roche), and sections were counterstained with Hoechst 33342 (Sigma). In situ hybridization was performed as described (2) with *Vegf*, *flk-1*, and *flt-1* probes (23).
11. T. P. Yamaguchi, D. J. Dumont, R. A. Conlon, M. L. Breitman, J. Rossant, *Development* **118**, 489 (1993).
12. D. J. Dumont et al., *Dev. Dyn.* **203**, 80 (1995).
13. P. Carmeliet et al., *Nature* **380**, 435 (1996).
14. N. Ferrara et al., *Nature* **380**, 439 (1996).
15. E9.5 embryos were minced into small fragments and cultured in individual wells on 48-well plates in Dulbecco's modified Eagle's medium containing 15% fetal calf serum, glutamine, penicillin, and streptomycin for 5 days. Cells were trypsinized and replated, and nonadherent cells were removed 1 hour later. For the VEGF analysis, 25,000 MEFs from individual embryos in passage 3 were plated on 24-well plates and cultured in normoxic (21% O₂) or hypoxic (1% O₂) conditions for 24 hours. Conditioned medium was removed and VEGF concentration was analyzed by enzyme-linked immunosorbent assay (ELISA) (R&D Systems). Remaining cells were lysed immediately in SDS sample buffer, subjected to SDS-PAGE analysis, and immunoblotted with antibodies to glucose transporter 1 (Chemicom).
16. J. A. Forsythe et al., *Mol. Cell. Biol.* **16**, 4604 (1996).
17. J. M. Gleadle, P. J. Ratcliffe, *Blood* **89**, 503 (1997).
18. J. R. Gnarr et al., *Proc. Natl. Acad. Sci. U.S.A.* **94**, 9102 (1997).
19. G. Siemeister et al., *Cancer Res.* **56**, 2299 (1996).
20. S. Pal, K. P. Claffey, H. F. Dvorak, D. Mukhopadhyay, *J. Biol. Chem.* **272**, 27509 (1997).
21. F. M. Giardiello et al., *Gastroenterology* **119**, 1447 (2000).
22. Y. Lallemand, V. Luria, R. Haffner-Krausz, P. Lonai, *Transgenic Res.* **7**, 105 (1998).
23. A. Kaipainen et al., *J. Exp. Med.* **178**, 2077 (1993).
24. We thank J. Partanen for discussions and reagents, P. Lonai for the PGK-Cre mice strain, and B. Tjäder and S. Räsänen for technical assistance. Supported by the Finnish Medical Foundation, Vuorisalo Fund, Orion-Farmos Research Foundation, Emil Aaltonen Foundation, Finnish Cancer Foundation, Ida Montin Foundation, and Academy of Finland. A.Y. and D.J.R. are in Helsinki Biomedical Graduate School, and N.K. is in the Helsinki Graduate School in Biotechnology and Molecular Biology.

30 April 2001; accepted 22 June 2001